



Journal of Applied Fluid Mechanics, Vol. 9, No. 4, pp. 1819-1827, 2016.
Available online at www.jafmonline.net, ISSN 1735-3572, EISSN 1735-3645.
DOI: 10.18869/acadpub.jafm.68.235.22833

Effect of Heat Transfer on Oscillatory Flow of Blood through a Permeable Capillary

A. Sinha

Department of Mathematics Yogoda Satsanga Palpara Mahavidyalaya, West Bengal-721458, India

Email: aniruddha.sinha07@gmail.com

(Received March 14, 2014; accepted October 18, 2015)

ABSTRACT

Of concern in the paper is a study on heat transfer in the unsteady magnetohydrodynamic (MHD) flow of blood through a porous segment of a capillary subject to the action of an external magnetic field. Nonlinear thermal radiation and velocity slip condition are taken into account. The time-dependent permeability and suction velocity are considered. The governing non-linear partial differential equations are transformed into a system of coupled non-linear ordinary differential equations using similarity transformations and then solved numerically using Crank-Nicolson scheme. The computational results are presented in graphical/tabular form and thereby some theoretical predictions are made with respect to the hemodynamical flow of blood in a hyperthermal state under the action of a magnetic field. Effects of different parameters are adequately discussed. The results clearly indicate that the flow is appreciably influenced by slip velocity and also by the value of the Grashof number. It is also observed that the thermal boundary layer thickness enhances with increase of thermal radiation.

Keywords: Magnetohydrodynamics; Thermal radiation; Slip velocity; Suction velocity.

1. INTRODUCTION

The literature of bio-mathematics has provided huge number of applications in medicine and biology. The application of MHD has reducing effect on the rate of flow of blood in human arterial system, which is useful in treatment of certain cardiovascular disorders such as brain-hemorrhage and hypertension etc. (Korchevskii and Marochnik 1965). Pulsed magnetic fields have been used to treat various conditions, such as soft-tissue injury (Wilson 1974), chronic pelvic pain (Varcaccio *et al.* 1995). Vardanyan (1973) explored the potential use of MHD principles in prevention and rational therapy of arterial hypertension, wherein he reported that a magnetic field applied in a direction transverse to an artery bears the potential to alter the flow rate of blood. Halder (1994) analyzed the effect of magnetic field on blood flow through an indented tube in presence of erythrocytes. A mathematical model for biomagnetic fluid dynamics, suitable for the description of the Newtonian blood flow under the action of an applied magnetic field has been proposed by Tzirtzilakis (2005).

Earlier studies on flow through porous media were mainly based upon the use of Darcy's law (Darcy 1856), which relates linearly the flow velocity to the pressure gradient across the porous medium. Later

developments on fluid flow through porous media led to different extensions of the Darcy law, such as the Forchheimer equation (Joseph *et al.* 1982) and the Brinkman equation (Brinkman 1947). Dash *et al.* (1996) employed the Brinkman equation to model the pathological blood flow when there is accumulation of fatty plaques of cholesterol in the lumen of an arterial segment and artery-clogging takes place by blood clots. They considered the clogged region as a porous medium and considered the permeability to be either constant or varying in the radial direction. Kumar *et al.* (2002) studied the unsteady laminar free convection flow of an electrically conducting fluid through a porous medium along a hot porous plate, where the suction velocity is time-dependent. However, none of these studies considered the oscillatory suction velocity of the fluid under the action of a magnetic field.

Misra *et al.* (2011) conducted a study concerning blood flow through a porous vessel where they considered no-slip condition at the vessel wall. It is well-known that a viscous fluid normally sticks to the boundary, that is, there is no slip of the fluid relative to the boundary. There are, however, many situations where there may be a partial slip between the fluid and the boundary. For many fluids, such as particulate fluids, the motion is still governed by the Navier-Stokes equations, but the usual no-slip condition at the boundary should be replaced by the

slip condition (Sinha and Misra 2014). Wang (2002) considered a problem involving partial slip by considering stagnation point flows.

Recently, heat transfer analysis have been received the attention (Srinivas and Gayathri 2009; Srinivas and Kothandapani 2008) due to its large number of applications in the processes like hemodialysis and oxygenation. Bio-heat is currently considered as heat transfer in the human body. In view of this thermosterapy and the human thermoregulation system (Srinivas and Kothandapani 2008), the model of bio-heat transfer in tissues has been attracted by the biomedical engineers. Radiation effect in blood flow is an important subject of research, because it has got significant applications in Biomedical engineering and several medical treatment methods, particularly in thermal therapeutic procedures. Sheikholeslami *et al.* (2014a) investigated effect of magnetic field on CuO-water nano fluid flow and heat transfer in an enclosure which is heated from below. They concluded that the enhancement in heat transfer increases as Hartmann number and heat source length increase but it decreases with increase of Rayleigh number. Sheikholeslami *et al.* (2014b) also studied natural convection heat transfer of Cu-water nanofluid in an enclosure with hot elliptic cylinder in presence of magnetic field. Several investigations has been carried out by some researchers (Ellahi *et al.* 2014;)cf. [19]-[25]) to examine heat transfer effect on different fluid models. The effect of radiative heat transfer on blood flow in a stenosed artery was studied theoretically by Prakash and Makinde (2011). Misra *et al.* (2010) reported theoretical estimates of blood flow in arteries during the therapeutic procedure of electromagnetic hyperthermia used for cancer treatment. Some relevant useful discussions are also available in that paper. Sharma *et al.* (2014) theoretically investigated the role of slip velocity on boundary layer flow of viscous fluid with heat transfer over an exponentially shrinking sheet in the presence of thermal radiation. Das *et al.* (2014) studied unsteady flow and heat transfer of a viscous incompressible, electrically conducting dusty fluid past vertical plate under the influence of a transverse magnetic field with a view to examine the combined effects of suction, heat absorption and ramped wall temperature.

The motivation of this paper is to study the influence of slip velocity on unsteady MHD flow as well as the associated problem on heat transfer in the presence of thermal radiation, in the case of blood flow through a porous capillary in a pathological state, where the capillary has turned into a porous medium due to accumulation of fats, cholesterol and blood clots. The analysis presented here pertains to a situation when the capillary is subjected to a time-dependent suction velocity. These aspects are paid due attention in this study. Moreover, the unsteady oscillatory behaviour of the fluid flow is studied here because of the reason that, due to the unsteady motion of the capillary wall/wall temperature, the flow of the fluid becomes unsteady. The problem is solved

numerically by an appropriate finite difference method. The study has the promise of significant application in electromagnetic therapy, which has gained much popularity in recent years in the treatment of cancer.

2. MATHEMATICAL ANALYSIS

Let us consider unsteady, two-dimensional flow and heat transfer of an incompressible electrically conducting fluid through a porous having time-dependent permeability in the presence of thermal radiation. The suction velocity is considered oscillatory. In the mathematical analysis that follows, we use Cartesian coordinates (x', y') , where the x' -axis is taken along the center line of the channel (see Fig. 1) and parallel to the channel surface, while the y' -axis is along in the transverse direction. The flow is considered symmetric about the x' -axis. The porous walls of the channel can be represented as $y' = h$ and $y' = -h$ (h being half-width of the channel). The permeability of the porous medium is considered to be $K' = K_0(1 + \varepsilon \sin(n't'))$, and the suction velocity is assumed to be $v' = v_0(1 + \varepsilon \sin(n't'))$, where K_0 is the constant permeability of the medium, $\varepsilon \ll 1$ is a small positive constant, n' is the frequency of oscillation, and $v_0 (> 0)$ is the scale of the suction velocity. As per experimental observation, blood is a conducting fluid. Hence under the action of the magnetic field, the flow of blood will be of magneto-hydrodynamic (MHD) nature. In the analysis, it is assumed that the magnetic Reynolds number is much less than unity so that the induced magnetic field is negligible in comparison to the applied magnetic field. We also incorporate the slip effect on the fluid flow.

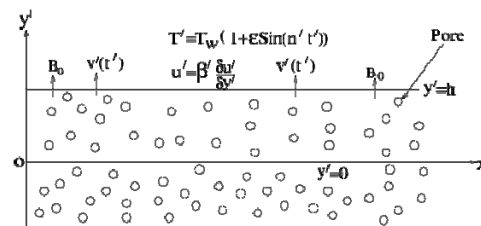


Fig. 1 Physical sketch of the problem.

With all the above-mentioned consideration, taking the usual Boussinesq approximation into account, the equations that govern the motion of the fluid may be listed as

$$\frac{\partial u'}{\partial x'} = 0, \tag{1}$$

$$\frac{\partial u'}{\partial t'} + v' \frac{\partial u'}{\partial y'} = \nu \frac{\partial^2 u'}{\partial y'^2} - \frac{u'}{K'} + g\beta(T' - T_w) - \frac{\sigma B_0^2}{\rho} u', \tag{2}$$

and

$$\frac{\partial T'}{\partial t'} + \nu \frac{\partial T'}{\partial y'} = \frac{k}{\rho c_p} \frac{\partial^2 T'}{\partial y'^2} - \frac{1}{\rho c_p} \frac{\partial q_r}{\partial y'} \quad (3)$$

where ν is the kinematic coefficient of viscosity, β is the coefficient of thermal expansion, g being the acceleration due to gravity, σ is the electrical conductivity, ρ is the fluid density, B_0 is the strength of the applied magnetic field, T_w is the initial temperature of the wall, k being the thermal conductivity, c_p is the specific heat at constant pressure and q_r is the radiative heat flux.

The relevant boundary conditions are

$$\frac{\partial u'}{\partial y'} = 0 \text{ and } \frac{\partial T'}{\partial y'} = 0 \quad \text{at } y = 0, \quad (4)$$

$$\begin{aligned} u' &= \beta \frac{\partial u'}{\partial y'} \text{ and } T' = T_w (1 + \varepsilon \sin(\eta t')) \\ \text{and} \quad \alpha y' &= h \end{aligned} \quad (5)$$

in which β' represents the slip length.

By using Rosseland approximation, the relative heat flux can be expressed as

$$q_r = -\frac{4\sigma^{\hat{a}}}{3k^{\hat{a}}} \frac{\partial T'^4}{\partial y'} \quad (6)$$

where $\sigma^{\hat{a}}$ is the Stefan-Boltzmann constant and $k^{\hat{a}}$ being the mean absorption coefficient.

To examine the unsteady flow regime adjacent to the sheet, the following transformations are invoked

$$\begin{aligned} u &= \frac{u'}{v_0}, T = \frac{T' - T_w}{T_w}, y = \frac{y'}{h}, t = \frac{t' v_0}{4h} \\ \text{and } n &= \frac{4n'h}{v_0} \end{aligned} \quad (7)$$

Substituting eqn. (7) into eqns. (2) and (3), we get the following set of equations:

$$\begin{aligned} \frac{1}{4} \frac{\partial u}{\partial t} + f(t) \frac{\partial u}{\partial y} &= \frac{1}{Re} \frac{\partial^2 u}{\partial y^2} - \frac{u}{Re k_p f(t)} \\ &- Ha^2 u + GrT, \end{aligned} \quad (8)$$

and

$$\begin{aligned} \frac{1}{4} \frac{\partial T}{\partial t} + f(t) \frac{\partial T}{\partial y} &= \frac{1}{RePr} [1 + Nr(1+T)^3] \\ \frac{\partial^2 T}{\partial y^2} + \frac{3Nr}{RePr} \left(\frac{\partial T}{\partial y}\right)^2 &(1+T)^2, \end{aligned} \quad (9)$$

where $f(t) = 1 + \varepsilon \sin(\eta t)$.

Also, the boundary conditions (4) and (5) give rise to

$$\frac{\partial u}{\partial y} = 0 \text{ and } \frac{\partial T}{\partial y} = 0 \quad \text{at } y = 0, \quad (10)$$

and

$$u = \beta \frac{\partial u}{\partial y} \text{ and } T = f(t) - 1 \quad \text{at } y = 1. \quad (11)$$

The non-dimensional parameters that appear in the transformed equations presented above are defined as

$Ha = \sqrt{\frac{\sigma}{\rho \nu_0}} h B_0$ the Hartman number,

$Re = \frac{v_0 h}{\nu}$ the Reynolds number, $Gr = \frac{g \beta T_w h^3}{v_0^2}$

the Grashof number, $k_p = \frac{K_0}{h^2}$ the permeability

parameter, $\beta = \frac{\beta'}{h}$ slip parameter, $Pr = \frac{\mu c_p}{k}$

Prandtl number and $Nr = \frac{16\sigma^{\hat{a}} T_w^3}{3k^{\hat{a}} k}$ the thermal radiation parameter.

3. NUMERICAL PROCEDURE

Equations (8) and (9) subjected to the boundary conditions (10) and (11) are solved numerically developing a suitable finite difference technique. The central difference scheme is employed to discretize the derivatives with respect to y in Eqs. (8) and (9) as

$$\frac{\partial P}{\partial y} = \frac{P_{i+1} - P_{i-1}}{2dy} + O(dy^2), \quad (12)$$

and

$$\frac{\partial^2 P}{\partial y^2} = \frac{P_{i+1} - 2P_i + P_{i-1}}{dy^2} + O(dy^2), \quad (13)$$

in which P stands for u and T .

The values of u and T at the mesh point y_i are denoted by u_i and T_i respectively and at the j th time-step, the same variables are denoted by u_i^j and T_i^j ,

where (8)

$$y_i = idy, \quad i = 1, 2, \dots, m$$

$$t_j = jdt, \quad j = 0, 1, \dots$$

Now applying Crank-Nicolson formula for the Eqs. (8) and (9), we have

$$A_i u_{i-1}^{j+1} + B_i u_i^{j+1} + C_i u_{i+1}^{j+1} = D_i^j, \quad (14)$$

and

$$A_2 T_{i-1}^{j+1} + B_2 T_i^{j+1} + C_2 T_{i+1}^{j+1} = D_{2i}^j, \quad (15)$$

with

$$A_1 = -r_1 - r_2, \quad B_1 = 1 + 2r_2 + 2dt \left(Ha^2 + \frac{1}{k_p Re_f} \right),$$

$$C_1 = r_1 - r_2,$$

$$D_{1i}^j = u_i^j + r_2(u_{i+1}^j - 2u_i^j + u_{i-1}^j) + 4dtGrT_i^j - 2dt \left(Ha^2 + \frac{1}{k_p Re_f} \right) u_i^j,$$

$$A_2 = -r_1 - \frac{r_2}{Pr} [1 + Nr(1 + T_i^j)^3],$$

$$B_2 = 1 + \frac{2r_2}{Pr} [1 + Nr(1 + T_i^j)^3],$$

$$C_2 = r_1 - \frac{r_2}{Pr} [1 + Nr(1 + T_i^j)^3],$$

$$D_{2i}^j = T_i^j + \frac{r_2}{Pr} [1 + Nr(1 + T_i^j)^3] (T_{i+1}^j - 2T_i^j + T_{i-1}^j) + \frac{3Nr}{Pr} (T_{i+1}^j - T_{i-1}^j)^2 (1 + T_i^j)^2,$$

$$r_1 = \frac{2fdt}{dy} \text{ and } r_2 = \frac{2dt}{Redy^2}.$$

where dy and dt are the mesh sizes along the space and time directions.

The system of linear Eqs. (14) and (15) are expressed as tri-diagonal system of equations which are solved by using Thomas algorithm.

For $j = 0$, the system of Eq. (14) may be written as

$$a_i u_{i-1}^1 + b_i u_i^1 + c_i u_{i+1}^1 = d_i^0, \quad \text{for } i = 1, 2, \dots, m \quad (16)$$

with

$$a_i = A_1, \quad \text{for } i = 2, 3, \dots, m$$

$$b_i = B_1, \quad \text{for } i = 1, 2, \dots, m$$

$$c_i = C_1, \quad \text{for } i = 1, 2, \dots, m - 1$$

$$d_i^0 = D_{1i}^0, \quad \text{for } i = 2, 3, \dots, m - 1$$

$$a_1 = 0, \quad c_m = 0, \quad d_1^0 = D_{11}^0 - A_1 u_0^0,$$

$$d_m^0 = D_{1m}^0 - C_1 u_m^0.$$

We further write

$$u_i^1 = p_i u_{i+1}^1 + q_i, \quad \text{for } i = 1, 2, \dots, m \quad (17)$$

and

$$u_{i-1}^1 = p_{i-1} u_i^1 + q_{i-1} \quad \text{for } i = 1, 2, \dots, m. \quad (18)$$

For $i = 1$, from the equation (16), one obtains

$$p_1 = -\frac{c_1}{b_1}, \quad q_1 = \frac{d_1^0}{b_1}.$$

Now eliminating u_{i-1}^1 from the Eq. (16) we get

$$u_i^1 = -\frac{c_i}{b_i + a_i p_{i-1}} u_{i+1}^1 + \frac{d_i^0 - a_i q_{i-1}}{b_i + a_i p_{i-1}}, \quad (19)$$

for $i = 1, 2, \dots, m$

in which

$$p_i = -\frac{c_i}{b_i + a_i p_{i-1}}, \quad i = 1, 2, \dots, m$$

$$q_i = \frac{d_i^0 - a_i q_{i-1}}{b_i + a_i p_{i-1}}, \quad i = 1, 2, \dots, m$$

Let us now take

$$u_{m+1}^1 = 0. \quad (20)$$

Using (20), from (17) we get

$$u_m^1 = q_m. \quad (21)$$

Now using Eq. (17), we can compute u_i^1 , for $i = m - 1, m - 2, \dots, 3, 2, 1$ in succession.

The same procedure can be adopted for any other value of j , that is for any instant of time.

Proceeding in a similar manner, we can solve (15) for temperature.

4. RESULTS AND DISCUSSION

The effect of slip velocity on MHD flow of blood and heat transfer in the presence of nonlinear thermal radiation over a porous capillary have been investigated. The system of coupled differential Eqs. (8) and (9) subject to the boundary conditions (10) and (11) are solved numerically by employing a finite difference scheme with Newton's linearization method described in the previous section. Computational study has been carried out with an aim to investigate the variation of different quantities of interest for the following ranges of values of the parameters involved (Misra *et al.* 2011; Prakash and Makinde 2011; Sinha and Misra 2012): $Ha = 0, 1, 2, 4$; $\beta = 0, 0.5, 1.0, 2.0$; $Gr = -10, -5, 5, 10$; $k_p = 0.05, 0.1, 0.15, 0.2$; $\varepsilon = 0.005, 0.01, 0.015, 0.02$, $Pr = 20, 21, 22, 23$; $Nr = 0, 1, 2, 4$; $n = 2$ and $Re = 1$.

Figures 2-7 respectively display the effects of Hartman number, Grashof number, slip parameter, permeability parameter, amplitude parameter and radiation parameter. Fig. 2 reveals that in the case of cooling of the capillary wall ($Gr > 0$), velocity decreases when the Hartman number increases.

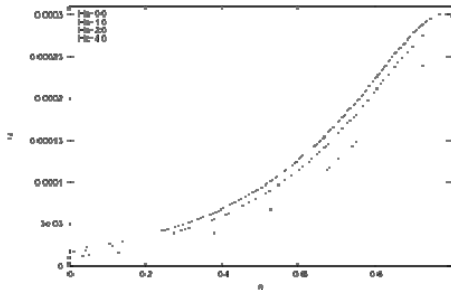


Fig. 2. Velocity distribution for different values of Hartmann number Ha when $Re = 1$, $Gr = 5$, $k_p = 0.1$, $Pr = 21$, $Nr = 1$, $\beta = 1.0$ and $\varepsilon = 0.005$.

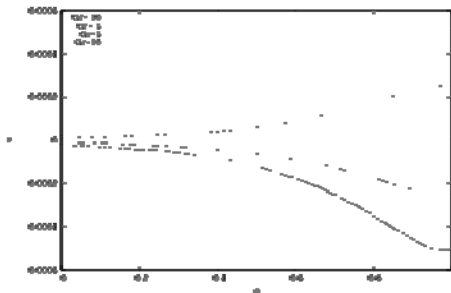


Fig. 3. Velocity distribution for different values of Grashof number Gr when $Re = 1$, $Ha = 2$, $k_p = 0.1$, $Pr = 21$, $Nr = 1$, $\beta = 1.0$ and $\varepsilon = 0.005$.

This observation agrees with the theory, because of the increase in magnetic parameter Ha , the Lorentz force increases. It is known that Lorentz force opposes the flow. This implies that if we increase in the strength of magnetic field, flow of blood will be impeded. One can also note that for any values of Hartman number, axial velocity increases upto near of the upper wall and after attaining its maximum value, it decreases. One can have an idea of the velocity distribution for both cooling of the wall ($Gr > 0$) and heating of the wall ($Gr < 0$) from Fig. 3. It may be noted that in the case of cooling, the velocity decreases as the Grashof number decreases, while in the case of heating, as the Grashof number decreases, the velocity increases. Fig. 4 reveals that velocity-slip at the wall of the capillary bears the potential to alter the velocity distribution to a significant extent. It is seen from the figure that for a fixed value of β , velocity oscillates with time. This figure also shows that blood velocity decreases as the slip factor increases. It may be noted that the velocity distribution is strongly influenced by the velocity-slip factor in the proximity of the wall but there is no such significant change in the vicinity of the axis of the capillary. It is revealed that the wall-slip effects bear the potential to arrest the velocity gradients in the interfacial region and also that such effects promote the advective transport of mobile ion through the capillary walls. Fig. 5 gives the variation in velocity with the height of the capillary.

This figure reveals that velocity of blood increases with the increase in wall permeability. It is worthwhile to further note that for the same permeability, the velocity increases with the height of the capillary and it attains maximum value at the near of the upper wall of the capillary. Figs. 6 and 7 give the variation of the blood velocity with amplitude parameter and the thermal radiation parameter respectively. From both figures, it is clearly seen that velocity of blood increases with both parameter ε and Nr .

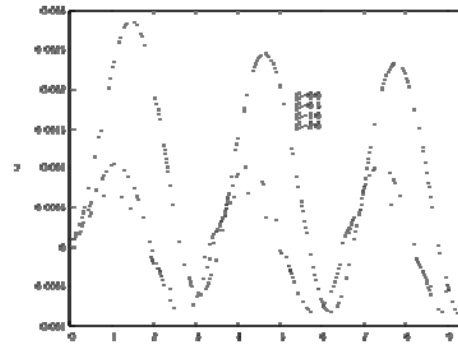


Fig. 4. The effect of slip parameter β on velocity profile when $Re = 1$, $Gr = 5$, $k_p = 0.1$, $Pr = 21$, $Nr = 1$, $\beta = 1.0$ and $\varepsilon = 0.005$.

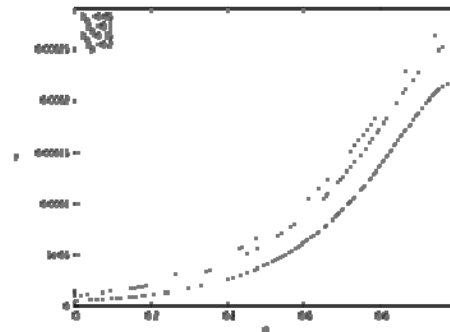


Fig. 5. Velocity distribution for different values of permeability parameter k_p when $Re = 1$, $Gr = 5$, $Ha = 2$, $Pr = 21$, $Nr = 1$, $\beta = 1.0$ and $\varepsilon = 0.005$.

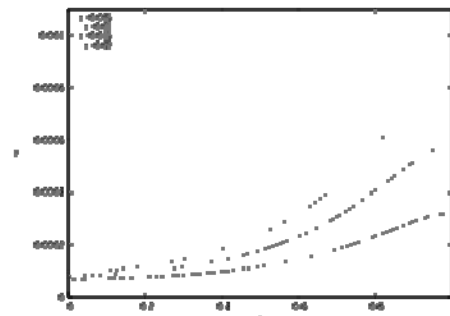


Fig. 6. Nature of velocity distribution for different values of ε when $Re = 1$, $Gr = 5$, $k_p = 0.1$, $Pr = 21$, $Nr = 1$, $\beta = 1.0$ and $Ha = 2$.

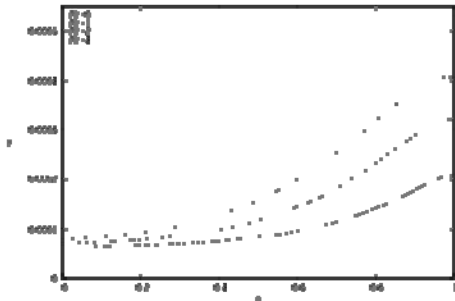


Fig. 7. Velocity distribution for different values of radiation parameter Nr when $Re = 1$, $Gr = 5$, $k_p = 0.1$, $Pr = 21$, $Ha = 2$, $\beta = 1.0$ and $\varepsilon = 0.005$.

Figs. 8-10 give some characteristic temperature profiles for different values of radiation parameter Nr , Prandtl number Pr and amplitude parameter \mathcal{E} respectively. Fig. 8 demonstrates the effect of thermal radiation on temperature profile T . This figure emphasizes that as thermal radiation increases during blood flow in capillaries, there is a significant rise in the thickness of boundary layer. Thereby the temperature of the boundary layer is enhanced by an appreciable extent. Fig. 9 presents the change in the temperature distribution in the boundary layer, when the Prandtl number (Pr) changes gradually. It shows that as the Prandtl number increases, the temperature of the boundary layer diminishes. This may be attributed to the fact that the thermal boundary layer thickness reduces with an increase in Prandtl number. Further, this figure indicates that the temperature gradient at the surface increases with a rise in Prandtl number. This implies that an increase in Prandtl number is accompanied by an enhancement of the heat transfer rate at the wall of the blood vessel. From Fig. 10 which elucidates the influence of the amplitude parameter (\mathcal{E}) on temperature distribution, it is revealed that the temperature of blood at any point of the flow medium increases with increasing value of \mathcal{E} . The skin-friction coefficient, defined as

$$C_f = \frac{2\tau_w}{\rho v_0^2} = -2Re \frac{1}{2}u'(1)$$

where $\tau_w = -\mu\left(\frac{\partial u}{\partial y}\right)_{y=h}$

is an important physical quantity that bears the potential to explore some vital information regarding problems such as the one under our present consideration.

The values of $-u'(1)$ for different sets of parameters are given in Table 1. The corresponding values of the local skin-friction coefficient can be computed by using the data presented in Table 1. With the increases in Gr , β , k_p and Nr , the skin-friction increases, while the increase in Ha/Pr gives rise to the reduction in the skin-

friction.

Another important characteristic of the present study is the local Nusselt number Nu , defined as

$$Nu = \frac{hq_w}{kT_w} = Re \frac{1}{2}\theta'(1)$$

where $q_w = k\left(\frac{\partial T}{\partial y}\right)_{y=h}$

The values of skin-friction and Nusselt number on the stretching wall, computed on the basis of the present study are presented in tabular form.

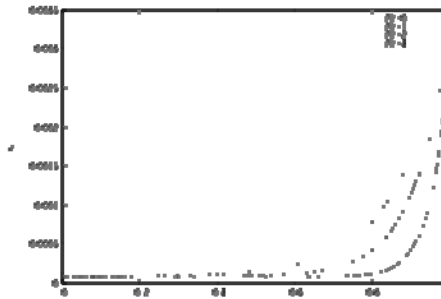


Fig. 8. Temperature distribution for different values of Nr when $Re = 1$, $Gr = 5$, $k_p = 0.1$, $Pr = 21$, $Ha = 2$, $\beta = 1.0$ and $\varepsilon = 0.005$.

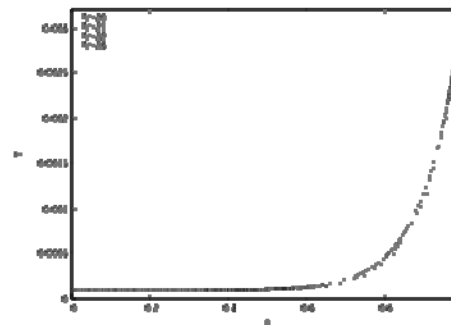


Fig. 9. Temperature distribution for different values of Pr when $Re = 1$, $Gr = 5$, $k_p = 0.1$, $Ha = 2$, $Nr = 1$, $\beta = 1.0$ and $\varepsilon = 0.005$.

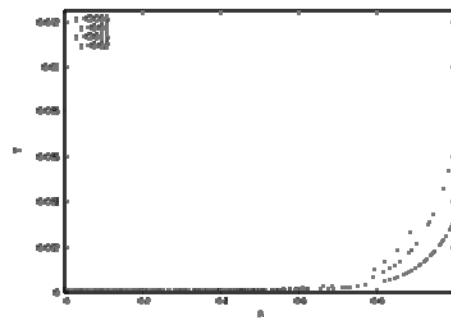


Fig. 10. Temperature distribution for different values of \mathcal{E} when $Re = 1$, $Gr = 5$, $k_p = 0.1$, $Pr = 21$, $Nr = 1$, $\beta = 1.0$ and $Ha = 2$.

Table 1 Distribution of $-u(1)$

| Ha | Gr | β | k_p | Pr | Nr | $-u'(1)$ |
|------|------|---------|-------|------|------|-------------|
| 2.0 | 5.0 | 1.0 | 0.1 | 21.0 | 1.0 | 0.00001812 |
| 3.0 | 5.0 | 1.0 | 0.1 | 21.0 | 1.0 | -0.0000188 |
| 4.0 | 5.0 | 1.0 | 0.1 | 21.0 | 1.0 | -0.00004827 |
| 2.0 | 10.0 | 1.0 | 0.1 | 21.0 | 1.0 | 0.00010535 |
| 2.0 | 20.0 | 1.0 | 0.1 | 21.0 | 1.0 | 0.0002798 |
| 2.0 | 5.0 | 0.5 | 0.1 | 21.0 | 1.0 | -0.0002959 |
| 2.0 | 5.0 | 2.0 | 0.1 | 21.0 | 1.0 | 0.00013234 |
| 2.0 | 5.0 | 1.0 | 0.15 | 21.0 | 1.0 | 0.0000378 |
| 2.0 | 5.0 | 1.0 | 0.2 | 21.0 | 1.0 | 0.00005026 |
| 2.0 | 5.0 | 1.0 | 0.1 | 20.0 | 1.0 | 0.000028725 |
| 2.0 | 5.0 | 1.0 | 0.1 | 22.0 | 1.0 | 0.00000834 |
| 2.0 | 5.0 | 1.0 | 0.1 | 21.0 | 2.0 | 0.000117224 |
| 2.0 | 5.0 | 1.0 | 0.1 | 21.0 | 4.0 | 0.00027226 |

Table 2 Distribution of $T(1)$

| Gr | Nr | Pr | $T'(1)$ |
|------|------|------|-------------|
| 5 | 1 | 21 | 0.032484904 |
| 10 | 1 | 21 | 0.03100677 |
| 5 | 2 | 21 | 0.022950606 |
| 5 | 1 | 20 | 0.031209597 |

From this table, one can have an idea of the variation in Nusselt number for different values of Grashof number Gr , radiation parameter (Nr) and Prandtl number (Pr). This table shows that increase in Pr , enhances the Nusselt number, while increase in Grashof number or radiation parameter leads to a reduction in local Nusselt number.

5. CONCLUDING REMARKS

A mathematical model formulated and analyzed has been motivated towards investigating the effect of non-linear thermal radiation on the flow and heat transfer in a capillary whose lumen being porous and wall permeable, when the system is subjected to the action of an external magnetic field. The porous matrix in the lumen of the capillary is supposed to be formed on account of some particular types of pathology of the capillary. The erythrocyte slip at the walls of the capillary has been duly account for.

The problem is formulated in terms of a non-linear boundary value problem that has been solved numerically by developing an appropriate finite difference scheme and using the Crank- Nicolson formula.

From this study, we can draw the following conclusions:

- (i) The blood velocity can be controlled by suitably adjusting (increasing/decreasing) the magnetic field strength/the slip coefficient. The results presented should be of sufficient interest to surgeons who usually want to keep the blood flow rate at a desired level during the entire surgical procedure.
- (ii) The velocity of blood along the axis of the capillary increases with a rise in permeability.
- (iii) The temperature of blood inside the boundary layer also reduces, if the Prandtl number increases.
- (iv) Thermal radiation bears the potential to bring about a significant change in the temperature field of the boundary layer. With a rise in thermal radiation, the thermal boundary layer thickness increases by an appreciable extent. This result is very much useful in the treatment of electromagnetic hyperthermia because the main objective of electromagnetic hyperthermia treatment is to rise the temperature of the cancerous tissues above $42^{\circ}C$.

ACKNOWLEDGMENT

The author (A.Sinha) is grateful to the NBHM, DAE, Mumbai for the financial support of this investigation.

REFERENCES

Akbar, N. S., M. Raza and R. Ellahi (2014). Influence of heat generation and heat flux on peristaltic flow with interacting nanoparticles. *The European Physical Journal Plus* 129, 1-15.

Brinkman, H. C. (1947). A calculation of the

- viscous force exerted by a flowing fluid on a dense swarm of particles. *Appl. Sci. Res. A* 1, 81-86.
- Darcy, H. R. P. G. (1856). *Les Fontaines Publiques de la Ville de Dijon*, Vector Dalmont.
- Das, M., B. K. Mahatha, R. Nandkeolyar, B. K. Mandal and K. Saurabh (2014). Unsteady Hydromagnetic Flow of a Heat Absorbing Dusty Fluid Past a Permeable Vertical Plate with Ramped Temperature. *J. Appl. Fluid Mech.* 7, 485-492.
- Dash, R. K., K. N. Mehta and G. Jayaraman (1996). Casson fluid flow in a pipe filled with homogeneous porous medium. *Int. J. Eng. Sci.* 34, 1146-1156.
- Ellahi, R., M. M. Bhatti and K. Vafai (2014). Effects of heat and mass transfer on peristaltic flow in a non-uniform rectangular duct. *Int. J. Heat Mass Trans.* 71, 706-719.
- Ellahi, R., X. W. ang and M. Hameed (2014). Effects of Heat Transfer and Nonlinear Slip on the Steady Flow of Couette Fluid by Means of Chebyshev Spectral Method. *Z. Naturforsch.* 69, 1-8.
- Halder, K. (1994). Effect of a Magnetic Field on Blood Flow Through an Indented Tube in the Presence of Erythrocytes. *Indian Journal of Pure and Applied Mathematics* 25, 345-352.
- Joseph, D. D., D. A. Nield and G. Papanicolaou (1982). Nonlinear equation governing flow in a saturated porous medium. *Water Resour. Res.* 18, 1049-1052.
- Korchevskii, M. and L. S. Marochnik (1965). Magnetohydrodynamic Version of Movement of Blood. *Biophysics* 10, 411-413.
- Kumar, A., B. Chand and A. Kaushik (2002). On unsteady oscillatory laminar free convection flow of an electrically conducting fluid through porous medium along a porous hot plate with time dependent suction in the presence of heat source/sink. *J. Acad. Math.* 24, 339-354.
- Misra, J. C., A. Sinha and G. C. Shit (2010). Flow of a biomagnetic viscoelastic fluid: application to estimation of blood flow in artery during electromagnetic hyperthermia, a therapeutic procedure for cancer treatment. *Appl. Math. Mech. (Eng. Educ.)* 31, 1405-1420.
- Misra, J. C., A. Sinha, and G. C. Shit (2011). A numerical model for the magnetohydrodynamic flow of blood in a porous channel. *J. Mech. Med. Biol.* 11, 547-562.
- Prakash, J. and O. D. Makinde (2011). Radiative heat transfer to blood flow through a stenotic artery in the presence of magnetic field. *Lat Am Appl. Res.* 41, 273-277.
- Rashidi, S., M. Dehghan, R. Ellahi, M. Riaz and M. T. Jamal-Abad (2015). Study of stream wise transverse magnetic field flow with heat transfer around an obstacle embedded in a porous medium. *Journal of Magnetism and Magnetic Materials* 378, 128-137.
- Sharma, R., A. Ishak, R. Nazar and I. Pop (2014). Boundary Layer Flow and Heat Transfer over a Permeable Exponentially Shrinking Sheet in the Presence of Thermal Radiation and Partial Slip. *J. Appl. Fluid Mech.* 7, 125-134.
- Sheikholeslami, M., D. D. Ganji, M. Y. Jadev and R. Ellahi (2014). Effect of thermal radiation on magnetohydrodynamics nanofluid flow and heat transfer by means of two phase model. *Journal of Magnetism and Magnetic Materials* 374, 36-43.
- Sheikholeslami, M., M. G. Bandpy, R. Ellahi and A. Zeeshan (2014). Simulation of MHD Cu-water nanofluid flow and convective heat transfer considering Lorentz forces. *Journal of Magnetism and Magnetic Materials* 369, 69-80.
- Sheikholeslami, M., M. G. Bandpy, R. Ellahi, M. Hassan and S. Soleimani (2014). Effects of MHD on Cu-water nanofluid flow and heat transfer by means of CVFEM. *Journal of Magnetism and Magnetic Materials* 349, 188-200.
- Sheikholeslami, M., R. Ellahi, H. R. Ashorynejad, G. Domairry and T. Hayat (2014). Effects of Heat Transfer in Flow of Nanofluids Over a Permeable Stretching Wall in a Porous Medium. *J. Comp. Theo. Nanoscience* 11, 486-496.
- Sheikholeslami, M., R. Ellahi, M. Hassan and S. Soleimani (2014). A study of natural convection heat transfer in a nanofluid filled enclosure with elliptic inner cylinder. *Int. J. Numer. Meth. Heat Fluid Flow* 24, 1906-1927.
- Sinha, A. and J. C. Misra (2014). MHD flow of blood through a dually stenosed artery: effects of viscosity variation, variable hematocrit and velocity-slip. *Canadian J. Chem. Engg.* 92, 23-31.
- Sinha, A., and J. C. Misra (2012). Numerical study of heat and mass transfer during oscillatory blood flow in diseased arteries in the presence of magnetic field. *Applied Mathematics and Mechanics (English Edition)* 33, 649-662.
- Srinivas, S. and M. Kothandapani (2008). Peristaltic Transport in an Asymmetric Channel with Heat Transfer-A Note. *International Communications of Heat and Mass Transfer* 35, 514-522.
- Srinivas, S. and R. Gayathri (2009). Peristaltic Transport of a Newtonian Fluid in a Vertical Asymmetric Channel with Heat Transfer and Porous Medium. *Applied Mathematical and Computer* 215, 185-196.
- Tzirtzilakis, E. E. (2005). A Mathematical Model for Blood flow in Magnetic field. *Physics of Fluids* 17, 077103.
- Varcaccio, G., C. Carriero and M. R. Loizzo (1995).

A. Sinha / *JAFM*, Vol. 9, No. 4, pp. 1819-1827, 2016.

Analgesic properties of electromagnetic field therapy in patients with chronic pelvic pain. *Clin Exp Obstet Gynecol* 22, 350-354.

Vardanyan, V. A. (1973). Effect of Magnetic Field on Blood Flow. *Biofizika* 18, 491-496.

Wang, C. Y. (2002). Stagnation flow with slip:

Exact solution of Navier-Stokes equations. *Chem. Eng. Sci.* 57, 3745-3747.

Wilson, D. H. (1974). Comparison of short wave diathermy and pulsed electromagnetic energy in treatment of soft tissue injuries. *Physiotherapy* 60, 309-310.